Randomly Punctured Spatially Coupled LDPC Codes

Mitchell, David G.M.; Lentmaier, Michael; Pusane, Ali E.; Costello Jr., Daniel J.

Published in:
[Host publication title missing]

2014

Randomly Punctured Spatially Coupled LDPC Codes

David G. M. Mitchell*, Michael Lentmaier†, Ali E. Pusane‡, and Daniel J. Costello, Jr.*
*Dept. of Electrical Engineering, University of Notre Dame, Notre Dame, Indiana, USA,
{david.mitchell, costello.2}@nd.edu
†Dept. of Electrical and Information Technology, Lund University, Lund, Sweden,
Michael.Lentmaier@eit.lth.se
‡Dept. of Electrical and Electronics Engineering, Bogazici University, Istanbul, Turkey,
ali.pusane@boun.edu.tr

***Abstract*—In this paper, we study random puncturing of protograph-based spatially coupled low-density parity-check (SC-LDPC) code ensembles. We show that, with respect to iterative decoding threshold, the strength and suitability of an LDPC code ensemble for random puncturing over the binary erasure channel (BEC) is completely determined by a single constant $\theta \geq 1$ that depends only on the rate and iterative decoding threshold of the mother code ensemble. We then use this analysis to show that randomly punctured SC-LDPC code ensembles display near capacity thresholds for a wide range of rates. We also perform an asymptotic minimum distance analysis and show that, like the SC-LDPC mother code ensemble, the punctured SC-LDPC code ensembles are also asymptotically good. Finally, we present some simulation results that confirm the excellent decoding performance promised by the asymptotic results.**

I. Introduction

It is often desirable in applications that experience changing channel conditions to be able to employ a variety of code rates. One method to achieve this is to *puncture* a low rate mother code. In this scheme, the transmitter punctures coded symbols, and, as a result of having fewer transmitted code symbols, the code rate is increased. It is assumed that the receiver knows the positions of the punctured symbols, so that both the punctured and transmitted symbols can be estimated during decoding. Coding schemes that use this technique are known as *rate-compatible punctured codes* [1]. Since the decoder for the mother code is used to decode the punctured codes, a variety of code rates can be achieved using the same decoding architecture by puncturing different numbers of symbols. Punctured low-density parity-check (LDPC) codes have been extensively studied in the literature (see, *e.g.*, [2], [3], [4], [5]).

Spatially coupled LDPC (SC-LDPC) codes are constructed by *coupling* together a series of L disjoint, or uncoupled, Tanner graphs into a single coupled chain, and they can be viewed as a type of LDPC convolutional code (LDPC-CC) [6], since spatial coupling is equivalent to introducing memory into the encoding process. SC-LDPC codes have been shown to combine excellent iterative decoding thresholds [7], [8] and good asymptotic minimum distance properties [9]. Moreover, it has been proven analytically for general memoryless binary-input symmetric-output (MBS) channels that the belief propagation (BP) decoding thresholds of a class of (J, K)-regular SC-LDPC code ensembles achieve the maximum a posteriori probability (MAP) decoding thresholds of the underlying (J, K)-regular LDPC block code ensembles, a phenomenon termed *threshold saturation* [8]. An algorithm to select particular puncturing patterns to construct robust rate-compatible LDPC-CCs was presented in [10].

In this paper, we consider random puncturing of protograph-based SC-LDPC code ensembles. We begin by showing that, with respect to the iterative decoding threshold, the strength and suitability of an LDPC code ensemble for random puncturing over the binary erasure channel (BEC) is completely determined by a single constant $\theta \geq 1$ that depends only on the rate and BEC threshold of the mother code ensemble. If $\theta = 1$, the punctured ensembles are capacity achieving for all higher rates, and if θ is close to 1, the punctured ensemble thresholds are close to capacity for all higher rates up to $1/\theta$. We then use this analysis to show that a variety of randomly punctured SC-LDPC code ensembles with large coupling length L display near capacity thresholds for a wide range of rates. We also perform an asymptotic minimum distance analysis and show that, like the SC-LDPC mother code ensemble, the punctured SC-LDPC code ensembles are also asymptotically good. Finally, we present some simulation results that demonstrate robust decoding performance of punctured SC-LDPC codes over a wide range of rates, confirming the excellent performance promised by the asymptotic results.

II. Randomly Punctured SC-LDPC Codes

A. Protograph-based LDPC Codes

A protograph [11] with *design rate* $R = 1 - n_c/n_v$ is a small bipartite graph that connects a set of n_v variable nodes to a set of n_c check nodes by a set of edges. The protograph can be represented by a parity-check or *base* biadjacency matrix $\mathbf{B}$, where $B_{x,y}$ is taken to be the number of edges connecting variable node v_y to check node c_x. The parity-check matrix $\mathbf{H}$ of a protograph-based LDPC block code can be created by replacing each non-zero entry in $\mathbf{B}$ by a sum of $B_{x,y}$ non-overlapping permutation matrices of size $M \times M$ and each zero entry by the $M \times M$ all-zero matrix. It is an important feature of this construction that each derived code inherits the degree distribution and graph neigborhood structure of the protograph. The ensemble of protograph-based LDPC codes with block length $n = Mn_v$ is defined by the set of matrices $\mathbf{H}$ that can be derived from a given protograph using all possible combinations of $M \times M$ permutation matrices. We denote the (J, K)-regular LDPC block code ensemble defined by the all-ones base matrix $\mathbf{B}$ of size $J \times K$ as $\mathcal{B}_{J,K}$.

Ensemble	Component base matrices
$\mathcal{C}_{3,4}(L)$	$\mathbf{B}_0 = \begin{bmatrix} 1 & 1 & 0 & 0 \\ 0 & 1 & 1 & 0 \\ 0 & 0 & 1 & 1 \end{bmatrix}, \mathbf{B}_1 = \begin{bmatrix} 0 & 0 & 1 & 1 \\ 1 & 0 & 0 & 1 \\ 1 & 1 & 0 & 0 \end{bmatrix}$
$\mathcal{C}_{3,6}(L)$	$\mathbf{B}_0 = \mathbf{B}_1 = \mathbf{B}_2 = \begin{bmatrix} 1 & 1 \end{bmatrix}$
$\mathcal{C}_{3,6,B}(L)$	$\mathbf{B}_0 = \begin{bmatrix} 1 & 1 \end{bmatrix}, \mathbf{B}_1 = \begin{bmatrix} 2 & 2 \end{bmatrix}$
$\mathcal{C}_{4,8}(L)$	$\mathbf{B}_0 = \mathbf{B}_1 = \mathbf{B}_2 = \mathbf{B}_3 = \begin{bmatrix} 1 & 1 \end{bmatrix}$
$\mathcal{C}_{4,8,B}(L)$	$\mathbf{B}_0 = \mathbf{B}_1 = \begin{bmatrix} 1 & 1 \end{bmatrix}, \mathbf{B}_2 = \begin{bmatrix} 2 & 2 \end{bmatrix}$
$\mathcal{C}_{3,9}(L)$	$\mathbf{B}_0 = \mathbf{B}_1 = \mathbf{B}_2 = \begin{bmatrix} 1 & 1 & 1 \end{bmatrix}$
$\mathcal{C}_{3,9,B}(L)$	$\mathbf{B}_0 = \begin{bmatrix} 1 & 1 & 1 \end{bmatrix}, \mathbf{B}_1 = \begin{bmatrix} 2 & 2 & 2 \end{bmatrix}$

TABLE I: SC-LDPC code ensemble component base matrices.

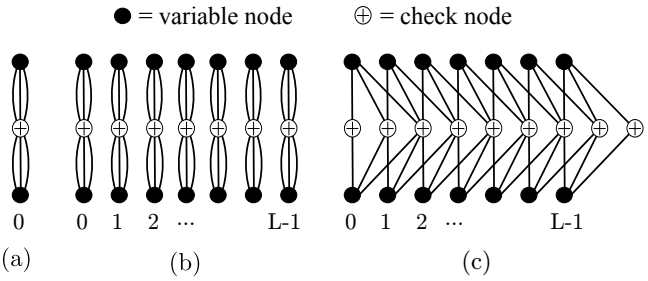

Fig. 1: Tanner graphs associated with (a) a $(3,6)$-regular LDPC block code protograph, (b) a chain of L uncoupled $(3,6)$-regular LDPC block code protographs, and (c) a chain of L spatially coupled $(3,6)$-regular LDPC block code protographs with coupling width $w = 2$.

B. Protograph-based SC-LDPC Codes

The base matrix of an SC-LDPC code ensemble with *coupling length* L is

$$\mathbf{B}_{[0,L-1]} = \begin{bmatrix} \mathbf{B}_0 & & & \\ \mathbf{B}_1 & \mathbf{B}_0 & & \\ \vdots & \mathbf{B}_1 & \ddots & \\ \mathbf{B}_w & \vdots & \ddots & \mathbf{B}_0 \\ & \mathbf{B}_w & & \mathbf{B}_1 \\ & & \ddots & \vdots \\ & & & \mathbf{B}_w \end{bmatrix}_{(L+w)b_c \times Lb_v}, \quad (1)$$

where w denotes the *coupling width* and the $b_c \times b_v$ *component base matrices* $\mathbf{B}_i$, $i = 0, 1, \ldots, w$, represent the edge connections from the b_v variable nodes at time t to the b_c check nodes at time $t+i$. An ensemble of SC-LDPC codes can then be formed from $\mathbf{B}_{[0,L-1]}$ using the protograph construction method described above. The design rate of the ensemble of SC-LDPC codes is

$$R_L = 1 - \frac{(L+w)b_c}{Lb_v}. \quad (2)$$

The ensembles and their component base matrices that we will refer to in this paper are given in Table I. Ensembles with a subscript "B" are referred to as "type B" ensembles where, by using entries larger than 1 in the component matrices $\mathbf{B}_i$, w is reduced and the rate increased for a given L. Fig. 1 illustrates the "edge-spreading" construction [9] of the protograph representing the SC-LDPC code ensemble $\mathcal{C}_{3,6}(L)$.

C. Puncturing Linear Codes

A linear code is *punctured* by removing a set of p columns from its generator matrix, which has the effect of reducing the codeword length from n to $n-p$. After puncturing a linear code with *puncturing fraction* $\alpha = p/n$, the resulting transmission rate will be equal to

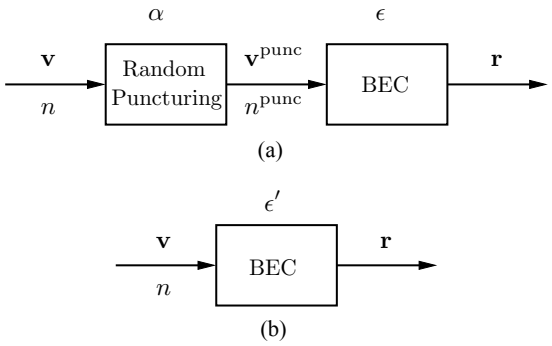

Fig. 2: (a) Block diagram illustrating random puncturing on the BEC, and (b) an equivalent BEC for random puncturing.

$$R(\alpha) = \frac{R}{1-\alpha}, \quad \alpha \in [0,1), \quad (3)$$

where $R(0) = R$ is the rate of the mother (unpunctured) code. A code can be punctured randomly or according to a particular pattern. It is assumed that the receiver knows the positions of the punctured bits, and the decoder estimates both the punctured and transmitted symbols during decoding.

III. Thresholds of Punctured LDPC Code Ensembles on the BEC

In this section, we consider the transmission of randomly punctured LDPC codes over the BEC. We begin by describing the channel model, showing that the problem can be modeled as two cascaded BECs or, equivalently, a single BEC with a modified erasure rate. We then determine the iterative BP decoding thresholds of punctured SC-LDPC code ensembles on the BEC.

A. Random Puncturing on the BEC

Consider puncturing a length n codeword $\mathbf{v}$ for transmission over a BEC with erasure probability ϵ. We assume that a fraction $\alpha = p/n$ of the code symbols are punctured, such that the transmitted codewords $\mathbf{v}^{\text{punc}}$ have length $n^{\text{punc}} = (1-\alpha)\cdot n$. After transmission over a channel with erasure probability ϵ, the received vector $\mathbf{r}$ will contain, on average, $\epsilon \cdot n^{\text{punc}}$ erased symbols and $(1-\epsilon)\cdot n^{\text{punc}}$ correct symbols. The receiver knows the positions of the punctured and erased symbols and proceeds to decode the overall code of length n.

Assuming that the positions of the punctured symbols are chosen randomly according to a uniform distribution, we can model the random puncturing as a BEC with erasure probability α. Combining the random puncturing channel together with the actual transmission channel, as shown in Fig. 2(a), one can model the transmission of randomly punctured codewords over the BEC as two cascaded BECs. This model is equivalent to a single BEC with crossover probability ϵ', as illustrated in Fig. 2(b). Since the number of correctly received symbols is equal for both models we obtain

$$(1-\epsilon')\cdot n = (1-\epsilon)\cdot n^{\text{punc}}, \quad (4)$$

which results in

$$\epsilon' = 1-(1-\epsilon)(1-\alpha). \quad (5)$$

B. Thresholds of Randomly Punctured LDPC Code Ensembles

Consider an arbitrary code ensemble of rate R with BEC iterative BP decoding threshold ϵ_{BP}. We are interested in the threshold $\epsilon_{\text{BP}}(\alpha)$ of the punctured code ensemble with rate $R(\alpha)$. In other words, we wish to know the channel parameter ϵ such that, after random puncturing with fraction α, we obtain an equivalent channel with parameter $\epsilon' = \epsilon_{\text{BP}}(0) = \epsilon_{\text{BP}}$. Using (5), we obtain

$$\epsilon_{\text{BP}}(0) = 1 - (1 - \epsilon_{\text{BP}}(\alpha))(1 - \alpha), \tag{6}$$

so that

$$\epsilon_{\text{BP}}(\alpha) = 1 - \frac{1 - \epsilon_{\text{BP}}(0)}{1 - \alpha} \tag{7}$$

or, using (3),

$$\epsilon_{\text{BP}}(\alpha) = 1 - \frac{1 - \epsilon_{\text{BP}}(0)}{R} \cdot R(\alpha) \ . \tag{8}$$

Note that (8) provides an explicit expression for the BP threshold of the punctured LDPC code ensemble with puncturing fraction α as a function of the target rate $R(\alpha) \geq R$, *i.e.*, for a given puncturing fraction α, the function $\epsilon_{\text{BP}}(\alpha)$ depends only on the threshold and the rate of the mother code ensemble. From (8), we define

$$\theta = \frac{1 - \epsilon_{\text{BP}}(0)}{R} \geq 1, \tag{9}$$

where we have equality if and only if the threshold of the mother code ensemble ϵ_{BP} is equal to the Shannon limit. The largest possible rate with puncturing is determined by the smallest non-negative threshold $\epsilon_{\text{BP}}(\alpha)$, which yields

$$R_{\text{max}} = R(\alpha = \epsilon_{\text{BP}}(0)) = \frac{1}{\theta} \ . \tag{10}$$

Thus, the maximum puncturing fraction α with a non-vanishing BP threshold is equal to the threshold $\epsilon_{\text{BP}}(0) = \epsilon_{\text{BP}}$ of the mother code. We refer to the range of rates $R(0) \leq R(\alpha) \leq R_{\text{max}}$ where the punctured code ensembles have non-negative thresholds as the *achievable rate range*.

Note the implications of (8) and (9): *θ determines the gap to capacity for all punctured code ensembles*. A large value of θ implies that the mother code ensemble has a threshold relatively far from the Shannon limit and the gap to capacity will grow quickly with increasing α; on the other hand, for a value of θ close to 1, the mother code ensemble has a threshold close to the Shannon limit and the gap to capacity will grow slowly with increasing α. In the extreme case where $\theta = 1$, *i.e.*, the threshold of the mother code ensemble is equal to the Shannon limit, then capacity is achieved for all punctured code ensembles with target rates $R(\alpha) \geq R$.

C. Numerical Threshold Results

Example 1 The $\mathcal{C}_{3,4}(L = 50)$ SC-LDPC code ensemble has BP threshold $\epsilon_{\text{BP}}(0) = 0.746$ and design rate $R(0) = 0.235$, which results in $\theta = 1.0809$. Similarly, the $\mathcal{C}_{3,6,B}(L = 50)$ SC-LDPC code ensemble has $\epsilon_{\text{BP}}(0) = 0.4881$ and $R(0) = 0.49$, which results in $\theta = 1.0447$. The underlying LDPC block code ensembles $\mathcal{B}_{3,4}$ and $\mathcal{B}_{3,6}$, with rates $R(0) = 0.25$ and $R(0) = 0.5$, have thresholds $\epsilon_{\text{BP}}(0) = 0.6474$ and $\epsilon_{\text{BP}}(0) = 0.4294$, resulting in $\theta = 1.4103$ and $\theta = 1.1411$, respectively. □

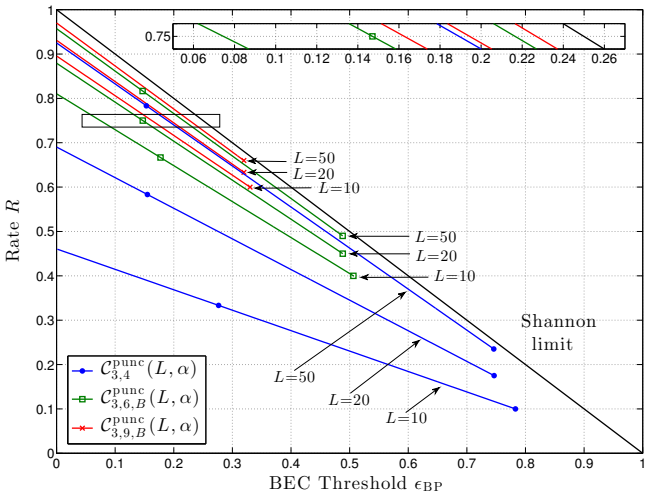

Fig. 3: BEC BP thresholds for the randomly punctured SC-LDPC code ensembles $\mathcal{C}^{\text{punc}}_{3,4}(L,\alpha)$, $\mathcal{C}^{\text{punc}}_{3,6,B}(L,\alpha)$, and $\mathcal{C}^{\text{punc}}_{3,9,B}(L,\alpha)$ for $L = 10, 20$, and 50 and a variety of puncturing fractions α.

Fig. 3 shows the calculated BEC BP thresholds for the randomly punctured SC-LDPC code ensembles $\mathcal{C}^{\text{punc}}_{3,4}(L,\alpha)$, $\mathcal{C}^{\text{punc}}_{3,6,B}(L,\alpha)$, and $\mathcal{C}^{\text{punc}}_{3,9,B}(L,\alpha)$ for $L = 10, 20$, and 50 and a variety of puncturing fractions α (dots, squares, and crosses) and also the thresholds predicted using (8) (solid lines). We observe that the predictions match the calculated thresholds. From $\epsilon_{\text{BP}}(\alpha) = 1 - \theta \cdot R(\alpha)$, we see that θ can be interpreted graphically as the slope of the parametrically defined line determining the position of the punctured thresholds $\epsilon_{\text{BP}}(\alpha)$ for all α. Since the mother code ensembles for these examples have thresholds close to capacity for large L, the corresponding values of θ are close to 1. Consequently, the thresholds of the punctured SC-LDPC code ensembles are close to capacity for all achievable rates $R(\alpha) \leq R_{\text{max}}$.

For the $\mathcal{C}_{3,4}(L)$ mother code ensembles, we obtain $\theta = 2.1710$, 1.1954, and 1.0809 for coupling lengths $L = 10$, 20, and 50, respectively. Consequently, for any common achievable rate, the $\mathcal{C}^{\text{punc}}_{3,4}(50,\alpha)$ code ensemble must have the best threshold. This can be observed in Fig. 3, where we see that the $\mathcal{C}^{\text{punc}}_{3,4}(50,0)$ threshold is closer to capacity than those of the $\mathcal{C}^{\text{punc}}_{3,4}(20,0)$ and $\mathcal{C}^{\text{punc}}_{3,4}(10,0)$ code ensembles, and the lines formed by the thresholds of the higher rate punctured ensembles are steeper in the negative direction as L increases. Similar conclusions are drawn when comparing the $\mathcal{C}_{3,6,B}(L)$ code ensembles and the $\mathcal{C}_{3,9,B}(L)$ code ensembles. Out of all the ensembles, we find that the $\mathcal{C}_{3,9,B}(50)$ mother code ensemble has the best θ and, consequently, for any common achievable rate, the punctured $\mathcal{C}^{\text{punc}}_{3,9,B}(50,\alpha)$ ensemble must have the best BP threshold. For example, rate $R = 0.75$ is highlighted in Fig. 3. From right to left, for appropriate values of α such that $R(\alpha) = 0.75$, the ordering of the ensembles is $\mathcal{C}^{\text{punc}}_{3,9,B}(50,\alpha)$, $\mathcal{C}^{\text{punc}}_{3,6,B}(50,\alpha)$, $\mathcal{C}^{\text{punc}}_{3,9,B}(20,\alpha)$, $\mathcal{C}^{\text{punc}}_{3,4}(50,\alpha)$, $\mathcal{C}^{\text{punc}}_{3,9,B}(10,\alpha)$, $\mathcal{C}^{\text{punc}}_{3,6,B}(20,\alpha)$, and $\mathcal{C}^{\text{punc}}_{3,6,B}(10,\alpha)$, precisely the ordering of increasing θ values of the mother code ensembles. (Note that the $\mathcal{C}^{\text{punc}}_{3,4}(10,\alpha)$ and $\mathcal{C}^{\text{punc}}_{3,4}(20,\alpha)$ ensembles cannot achieve $R(\alpha) = 0.75$.)

	θ				
Ensemble	$L=20$	$L=50$	$L=\infty$	Ensemble	θ
$\mathcal{C}_{3,4}(L)$	1.1954	1.0810	1.0161	$\mathcal{B}_{3,4}$	1.4103
$\mathcal{C}_{3,6}(L)$	1.1372	1.0664	1.0237	$\mathcal{B}_{3,6}$	1.1411
$\mathcal{C}_{3,6,B}(L)$	1.0776	1.0447	1.0237		
$\mathcal{C}_{4,8}(L)$	1.1817	1.0687	1.0046	$\mathcal{B}_{4,8}$	1.2331
$\mathcal{C}_{4,8,B}(L)$	1.1162	1.0465	1.0046		
$\mathcal{C}_{3,9}(L)$	1.0741	1.0414	1.0205	$\mathcal{B}_{3,9}$	1.0757
$\mathcal{C}_{3,9,B}(L)$	1.0467	1.0309	1.0205		

TABLE II: Calculated values of θ for various mother SC-LDPC and LDPC block code ensembles.

We also see that, as we increase L, the gap to capacity for the SC-LDPC code ensembles considered is monotonically decreasing in such a way that θ is monotonically decreasing (improving). Table II displays calculated values of θ for various mother SC-LDPC and LDPC block code ensembles. We find that the type B ensembles, with smaller coupling width and thus less rate loss for finite L, have better values of θ, but this advantage disappears as $L \to \infty$. Comparing the $(3, K)$ ensembles, we find that, for large L, the $\mathcal{C}_{3,4}(L)$ ensemble has the smallest value of θ and consequently randomly puncturing this ensemble will result in the best thresholds - even for high rates. (In Fig. 3, we considered a maximum value of $L = 50$, where the $\mathcal{C}_{3,9,B}(50)$ ensemble had the smallest value of θ but, for a sufficiently large L, the $\mathcal{C}^{\text{punc}}_{3,4}(L, \alpha)$ ensembles will outperform the $\mathcal{C}^{\text{punc}}_{3,9,B}(L, \alpha)$ ensembles.) We should note, however, that the value of θ depends closely on the particular "edge spreading" used to construct the protograph. This gives rise to the interesting question of what is the best edge spreading and (J, K) pair that minimizes θ for a fixed J? Increasing the graph density is known to result in SC-LDPC mother code ensembles with thresholds approaching capacity for large L, and we observe that the $(4, 8)$ ensembles correspondingly have θ values close to 1 for large L. Finally, we note that the LDPC block code ensembles $\mathcal{B}_{J,K}$ have large θ values that grow with increasing density (recall that θ determines the additive gap to capacity $\epsilon_{\text{Sh}} - \epsilon_{\text{BP}} = (\theta - 1) \cdot R$ and that ϵ_{BP} worsens as the density increases for fixed R).

D. Remarks

- The results detailed in this section are not specific to SC-LDPC code ensembles. More generally, if one can find a capacity approaching or capacity achieving code ensemble then it will have a θ value close to, or equal to, 1 and it will be well suited to random puncturing as discussed above. In fact, similar statements regarding capacity achieving LDPC code ensembles on the BEC with puncturing have been made before (see *e.g.*, [4], [12]). However, the threshold saturation of SC-LDPC code ensembles results in simple (J, K)-regular code ensembles with thresholds close to capacity and small θ values. Without spatial coupling, one would have to design an optimized capacity approaching block code ensemble to obtain a good value of θ, or accept a bad θ with a (J, K)-regular LDPC block code ensemble.
- Designing optimized irregular mother LDPC block code ensembles to obtain a good θ for a given R is likely to result in an ensemble with poor minimum distance properties. In addition to having thresholds close to capacity and correspondingly good θ values, (J, K)-regular SC-LDPC mother code ensembles are known to have linear minimum distance growth [9]. In Section IV, we show that this property carries over to randomly punctured SC-LDPC code ensembles.
- We saw that the derivation of the thresholds of randomly punctured LDPC code ensembles is independent of the decoding algorithm or the structure of the mother code. To determine thresholds for all punctured ensembles of rate $R \leq R(\alpha) \leq R_{\text{max}}$, we only require the threshold and the rate of the mother code. A similar argument can be made for the threshold of the MAP decoder, for example. In this case, everything follows through and simply leads to a different θ.

IV. Minimum Distance Growth Rates of Punctured SC-LDPC Code Ensembles

In [9], it was shown that ensembles of $\mathcal{C}_{J,K}(L)$ SC-LDPC codes are *asymptotically good*, in the sense that the minimum distance typical of most members of the ensemble is at least as large as $\delta_{\min} \cdot n$, where $\delta_{\min} > 0$ is the *minimum distance growth rate* of the ensemble. In this section, we investigate the distance properties of randomly punctured SC-LDPC code ensembles.[1]

We define the *asymptotic spectral shape* of a linear code ensemble as

$$r(\delta) = \limsup_{n \to \infty} \frac{1}{n} \ln(A_{\lfloor \delta n \rfloor}), \tag{11}$$

where $\delta = d/n$ is the normalized Hamming distance d, $n \in \mathbb{N}$ is the block length, and A_d is the ensemble weight enumerator. The spectral shape function can be used to test if an ensemble is asymptotically good. A technique to calculate the asymptotic spectral shape $r(\delta)$ for protograph-based block LDPC code ensembles was presented in [13]. Given the spectral shape function $r(\delta)$ of an asymptotically good code ensemble, the expected spectral shape of the randomly punctured code ensemble can be obtained as [14]

$$r^{\text{punc}}(\delta) = \frac{1}{1-\alpha} \left(\max_{0 \leq \lambda \leq 1} \left\{ \lambda H\left(\frac{(1-\alpha)\delta}{\lambda} \right) + (1-\lambda) H\left(\frac{\alpha + (1-\alpha)\delta - \lambda}{1-\lambda} \right) + r(\lambda) \right\} - H(\alpha) \right), \tag{12}$$

where $\alpha = p/n$ is the fraction of punctured bits, and $H(\delta) = -(1-\delta)\ln(1-\delta) - \delta \ln(\delta)$ is the binary entropy function.

Fig. 4 shows the asymptotic spectral shape functions for the $\mathcal{C}^{\text{punc}}_{3,6}(L = 8, \alpha)$ ensembles for several puncturing fractions α. The spectral shape of the mother code corresponding to $\alpha = 0$ is highlighted as a bold red curve. Also shown are the asymptotic spectral shape functions for random codes with the corresponding rate $R(\alpha)$ calculated using (see [15])

$$r(\delta) = H(\delta) - (1 - R(\alpha)) \ln(2). \tag{13}$$

We observe that the $\mathcal{C}^{\text{punc}}_{3,6}(8, \alpha)$ code ensembles are asymptotically good and have large minimum distance growth rates $\delta_{\min}(\alpha)$. (Minimum distance growth rates for selected values of α are shown in Table III.) The mother code ensemble

[1] We restrict our discussion to $\mathcal{C}^{\text{punc}}_{3,6}(L, \alpha)$ ensembles in this section; however, similar behavior is observed for other J and K values.

α	$R(\alpha)$	$\delta_{\min}(\alpha)$
0	0.375	0.0324
0.01	0.378	0.0323
0.1	0.416	0.0314
0.25	0.5	0.0293
0.3	0.535	0.0283
0.4	0.625	0.0249

TABLE III: Minimum distance growth rates of randomly punctured SC-LDPC code ensembles $\mathcal{C}_{3,6}^{\text{punc}}(L=8,\alpha)$.

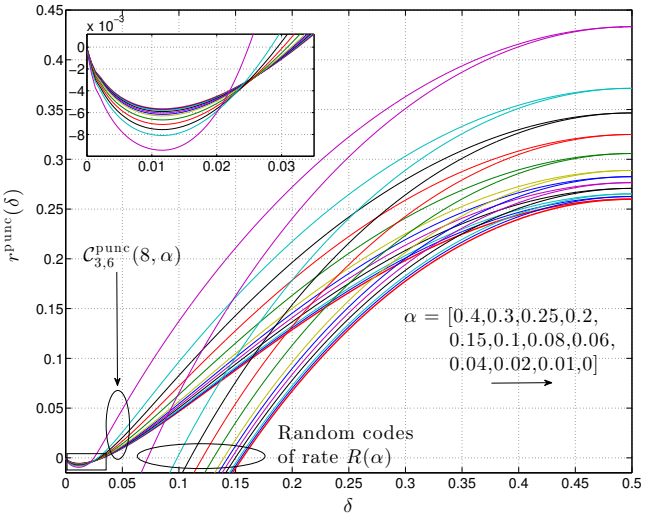

Fig. 4: Spectral shape functions of randomly punctured SC-LDPC code ensembles $\mathcal{C}_{3,6}^{\text{punc}}(L=8,\alpha)$ and random codes of the corresponding rate $R(\alpha)=0.375/(1-\alpha)$.

$\mathcal{C}_{3,6}^{\text{punc}}(8,0)$ has rate $R(0)=0.375$ and minimum distance growth rate $\delta_{\min}(0)=0.0324$. As α increases, the design rate $R(\alpha)=0.375/(1-\alpha)$ increases and the minimum distance growth rates decrease.[2] We observe moderate losses in minimum distance growth rate for the selected range of α (both the rate increase and distance growth rate decrease are superlinear). For example, puncturing 1% of the variable nodes results in a minimum distance growth rate decrease of 0.3% and puncturing 25% of the nodes results in a decrease of 9.5%, while the rates increase by 0.8% and 33.3%, respectively. Regarding the latter point, we note that the resulting design rate is $R(0.25)=0.5$ and the minimum distance growth rate is larger than that of the (equal rate) underlying $(3,6)$-regular LDPC block code ensemble $\delta_{\min}=0.023$.

Fig. 5 shows the minimum distance growth rates for mother SC-LDPC code ensembles $\mathcal{C}_{3,6}(L)$ and punctured SC-LDPC code ensembles $\mathcal{C}_{3,6}^{\text{punc}}(L,\alpha)$ for $L=3,4,5,6,7,8,10,12,14$ and a variety of puncturing fractions α. For a given L, each family of punctured ensemble $\mathcal{C}_{3,6}^{\text{punc}}(L,\alpha)$ displays the same behavior described above for $L=8$: the design rate increases and the minimum distance growth rates decrease with puncturing fraction α. We remark that SC-LDPC code ensembles provide a significant amount of flexibility for the

[2]If the puncturing fraction α is increased beyond a certain critical value, the asymptotic spectral shape function is no longer smooth. This observation is consistent with the emergence of "hook-like loops" in the spectral shapes of randomly punctured Gallager LDPC code ensembles for large α [14].

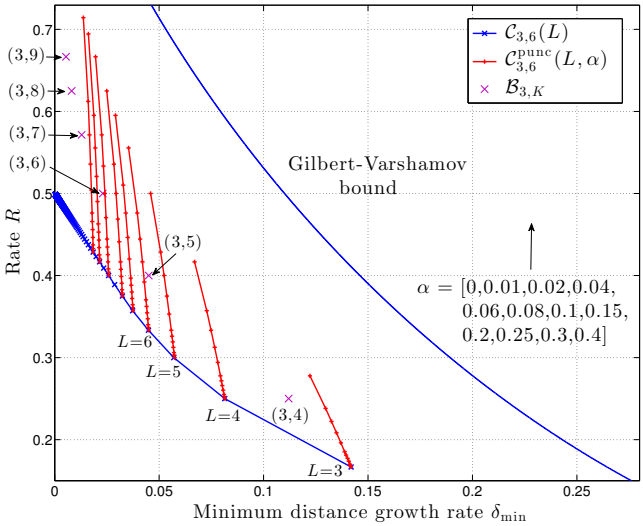

Fig. 5: Minimum distance growth rates for SC-LDPC code ensembles $\mathcal{C}_{3,6}(L)$ and punctured SC-LDPC code ensembles $\mathcal{C}_{3,6}^{\text{punc}}(L,\alpha)$ for $L=3,4,5,6,7,8,10,12,14$ and a variety of puncturing fractions α. Also shown for comparison are the minimum distance growth rates for (J,K)-regular LDPC-BC ensembles $\mathcal{B}_{J,K}$ and the Gilbert-Varshamov bound.

code designer. By varying L and α, for a single code design, a large variety of rates is achievable with varying minimum distance growth rates and thresholds. Also note that the trade-offs observed for the mother SC-LDPC code ensembles in [9] are also evident for randomly punctured ensembles: θ improves with increasing L (indicating better thresholds for all achievable rates), whereas the minimum distance growth rates decrease for any α with increasing L.

Due to the computational complexity of evaluating the asymptotic spectral shape function of SC-LDPC code ensemble protographs with large L, we have only presented numerical results for small L. However, we expect the trend in behavior observed for the values of L considered above to continue for large L: as the puncturing fraction α increases from 0, the minimum distance growth rates $\delta_{\min}(\alpha)$ decrease from $\delta_{\min}(0)$ and the ensemble design rates $R(\alpha)$ increase from $R(0)$. Note that, for large values of L, such as those considered in Section III, the gap to capacity of the mother code is decreasing and θ is improving. We expect that for a given large L in Fig. 5, the minimum distance growth rates $\delta_{\min}(\alpha)$ of $\mathcal{C}_{3,6}^{\text{punc}}(L,\alpha)$ can be approximated by a line originating from $\delta_{\min}(0)$, with decreasing (steeper and negative) slope as L increases (where, for a given $R(\alpha)$, $\delta_{\min}(\alpha)$ decreases as L increases). Consequently, as L increases, we observe a continuing trade-off of improving iterative decoding thresholds with decreasing minimum distance growth rates for all randomly punctured SC-LDPC code ensembles

V. Simulation Results

The bit erasure rate (BER) performance of randomly punctured SC-LDPC codes transmitted over the BEC was also investigated via computer simulations. A mother code with code length $n=50,000$ was drawn from the ensemble $\mathcal{C}_{3,6,B}(L=50)$ with protograph lifting factor $M=500$. This code has a rate of $R_{50}=0.49$. The code rate was increased

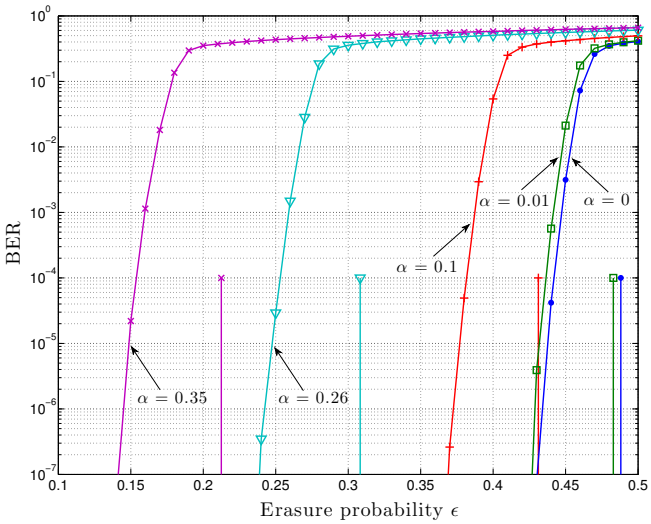

Fig. 6: BEC decoding error performance of randomly punctured SC-LDPC codes drawn from $\mathcal{C}^{\text{punc}}_{3,6,B}(50,\alpha)$ with protograph lifting factor $M = 500$. Also shown for comparison are the BP thresholds for the punctured SC-LDPC code ensembles $\mathcal{C}^{\text{punc}}_{3,6,B}(50,\alpha)$.

by randomly puncturing 5, 50, 130, and 175 out of every 500 variable nodes ($\alpha = 0.01, 0.1, 0.26$, and 0.35, respectively), yielding code rates of $R(0.01) = 0.495$, $R(0.1) = 0.544$, $R(0.26) = 0.662$, and $R(0.35) = 0.754$, respectively. The error performance of these codes was obtained using a sliding window decoder [7] with window size $W = 8$ and performing a maximum of $I = 10$ iterations in each window position. The results for these codes are presented in Fig. 6.

We observe excellent decoding performance from the punctured SC-LDPC codes of varying rates, with each code displaying a gap from its respective iterative decoding threshold of approximately 0.05 to 0.06 at a BER of 10^{-5}, for only a moderate lifting factor $M = 500$ and a resulting decoding latency of $2WM = 8000$ bits. We expect this gap to decrease as the lifting factor M is increased. Moreover, recall from Fig. 3 that, since $\theta = 1.0447$, the gap to capacity for the punctured thresholds is small and increases slowly as α, and correspondingly the rate $R(\alpha)$, increases. We note that it appears that the gap between the simulated decoding performance and the corresponding threshold increases slightly as α increases, which should be expected for a finite length code; however, the increase is small, demonstrating robust decoding performance for punctured SC-LDPC codes over a large range of rates. Finally, we note that we do not see any indication of an error-floor down to a BER of 10^{-7} for codes drawn from these asymptotically good code ensembles.

VI. Concluding Remarks

In this paper, we have studied random puncturing of protograph-based SC-LDPC code ensembles. We showed that, over the BEC, transmission of a randomly punctured code ensemble can be modeled as two cascaded BECs or, equivalently, a single BEC with a modified erasure rate. We also showed that, with respect to iterative decoding threshold, the strength and suitability of an LDPC code ensemble for random puncturing over the BEC is completely determined by a single constant $\theta \geq 1$ that depends only on the rate and the BP threshold of the mother code ensemble. If $\theta = 1$, the punctured ensembles are capacity achieving for all higher rates, and if θ is close to 1, the punctured ensemble thresholds are close to capacity for all higher rates up to $1/\theta$. We then used this analysis to show that randomly punctured SC-LDPC code ensembles with large coupling length L display near capacity thresholds over a wide range of rates. We also performed an asymptotic minimum distance analysis and showed that, like the SC-LDPC mother code ensemble, the punctured SC-LDPC code ensembles are also asymptotically good. Finally, we presented some simulation results that confirm the excellent decoding performance promised by the asymptotic results.

Acknowledgment

This work was partially supported by NSF Grant CCF-1161754 and TUBITAK Grant 111E276.

References

[1] J. Hagenauer, "Rate-compatible punctured convolutional codes (RCPC codes) and their applications," *IEEE Transactions on Communications*, vol. 36, no. 4, pp. 389–400, Apr. 1988.

[2] J. Ha, J. Kim, and S. W. McLaughlin, "Rate-compatible puncturing of low-density parity-check codes," *IEEE Transactions on Information Theory*, vol. 50, no. 11, pp. 2824–2836, Nov. 2004.

[3] J. Ha, J. Kim, D. Klinc, and S. W. McLaughlin, "Rate-compatible punctured low-density parity-check codes with short block lengths," *IEEE Transactions on Information Theory*, vol. 52, no. 2, pp. 728–738, Feb. 2006.

[4] H. Pishro-Nik and F. Fekri, "Results on punctured low-density parity-check codes and improved iterative decoding techniques," *IEEE Transactions on Information Theory*, vol. 53, no. 2, pp. 599–614, Feb. 2007.

[5] T. Van Nguyen, A. Nosratinia, and D. Divsalar, "The design of rate-compatible protograph LDPC codes," *IEEE Transactions on Communications*, vol. 60, no. 10, pp. 2841–2850, Oct. 2012.

[6] A. Jiménez Felström and K. Sh. Zigangirov, "Time-varying periodic convolutional codes with low-density parity-check matrices," *IEEE Transactions on Information Theory*, vol. 45, no. 6, pp. 2181–2191, Sept. 1999.

[7] M. Lentmaier, A. Sridharan, D. J. Costello, Jr., and K. Sh. Zigangirov, "Iterative decoding threshold analysis for LDPC convolutional codes," *IEEE Transactions on Information Theory*, vol. 56, no. 10, pp. 5274–5289, Oct. 2010.

[8] S. Kudekar, T. Richardson, and R. Urbanke, "Spatially coupled ensembles universally achieve capacity under belief propagation," *IEEE Transactions on Information Theory*, vol. 59, no. 12, pp. 7761–7813, Dec. 2013.

[9] D. G. M. Mitchell, M. Lentmaier, and D. J. Costello, Jr., "Spatially Coupled LDPC Codes Constructed from Protographs," submitted to the *IEEE Transactions on Information Theory*. [Online]: http://arxiv.org/abs/1407.5366.

[10] H. Zhou, D. G. M. Mitchell, N. Goertz, and D. J. Costello, Jr., "Robust rate-compatible punctured LDPC convolutional codes," *IEEE Transactions on Communications*, vol. 61, no. 11, pp. 4428–4439, Nov. 2013.

[11] J. Thorpe, "Low-density parity-check (LDPC) codes constructed from protographs," Jet Propulsion Laboratory, Pasadena, CA, INP Progress Report 42-154, Aug. 2003.

[12] C.-H. Hsu and A. Anastasopoulos, "Capacity-achieving codes with bounded graphical complexity and maximum likelihood decoding," *IEEE Transactions on Information Theory*, vol. 56, no. 3, pp. 992–1006, Mar. 2010.

[13] D. Divsalar, S. Dolinar, C. Jones, and K. Andrews, "Capacity-approaching protograph codes," *IEEE Journal on Selected Areas in Communications*, vol. 27, no. 6, pp. 876–888, Aug. 2009.

[14] E. C. Boyle and R. J. McEliece, "Asymptotic weight enumerators of randomly punctured, expurgated and shortened code ensembles," in *Proc. Allerton Conference*, Monticello, IL, Sept. 2008.

[15] R. G. Gallager, "Low-density parity-check codes," Ph.D. dissertation, Massachusetts Institute of Technology, Cambridge, MA, 1963.